

NO<sub>x</sub> .

### Adsorption-Desorption and Surface Reactivity of NO<sub>x</sub> on Chemically Modified Activated Carbon

Young-Whan Lee, Hyun-Jin Kim<sup>\*</sup>, Seung-Jun Son<sup>\*</sup>, Dae-Ki Choi<sup>\*</sup>, Jin-Won Park  
 Dept. of Chemical Engineering, Yonsei University  
 Environment and Process Technology Div., KIST<sup>\*</sup>

#### Introduction

Over the recent several years, development of surface modified activated carbon served as a springboard for improving the existing activated carbon (GAC). Several researchers have developed a diversity of SMAC over a couple of years by applying a number of different technologies to modify surface of GAC. Such SMAC proved to have far superior adsorption capacity against many other substances such as NO<sub>x</sub>, that is less adsorptive to GAC, as well as environment-polluting hazardous gases, which have many boiling points or low critical temperatures. As for other advantages, SMAC has high adsorption capacity even in the range from 100°C to 150°C, i.e. the temperature at which ordinary combustion flue gas is usually treated. In addition, SMAC enables desorption and regeneration at low temperature while it does not necessitate any additives. Despite the advantages described as above, SMAC still needs to undergo significant improvement via more systematic and advanced technologies in order to reach perfect process.

Understanding of adsorption/desorption behaviors and surface reaction mechanism may be integral to economical and efficient operation of adsorption process. Adsorption onto SMAC, in particular, accompanies not only physical adsorption but also chemical adsorption with adsorbate, which makes desorption process of SMAC more complicated when compared to desorption process of GAC. Desorption process requires surface chemical information on molecular ions of adsorbate distributed on the surface. However, the previous researches lacked study of these aspects. Therefore, this study investigated a typical behavior that appears when SMAC is used to examine adsorption at different bed depths at the temperature of 100°C and the subsequent desorption by adjusting the temperature upward. Furthermore, this study analyzed various surface characteristics using TGA-DSC, SEM, EPMA-EDS, ToF-SIMS and SIMS depth profiles in order to collect concrete data concerning surface reaction mechanism and characteristics of molecular ion distribution on the surface after adsorption and desorption.

#### Experimental Section

Coconut shell based activated carbon is used as adsorbent. SMAC is synthesized using the wet impregnation techniques. The detailed method for manufacturing step of adsorbent is described in our previous papers. The first experimental step is a heat treatment of SMAC to 10-100°C in the presence of He. The second step is the NO<sub>x</sub> adsorption in the presence of O<sub>2</sub>. In the third step for cooling down the sample to 10°C. Then, after maintaining to the temperature for 30min, a temperature programmed desorption (TPD) experiment is done in He at 5°C/min up to 600°C. The fixed-bed adsorption and desorption columns were a 316 stainless steel tube, with an inside diameter of 10.9 mm and a length of 400 mm. Inside the columns, steel mesh was placed in the upper and lower extremities of the adsorbent to support the samples and minimize channeling phenomenon. The temperature of the column was maintained with an electric furnace located at its outer wall. For the system line, the temperature was maintained by using a heat band and heat insulating material and was regulated with a proportional-integral-differential (PID) temperature controller. The temperature was measured by connecting a K-type thermocouple (Omega Engineering Inc.) located inside the line and connected to a recorder. Each certified 5000 ppm NO<sub>2</sub>/N<sub>2</sub> was diluted to the desired concentration range of 500 ppm via a mass flow controller (Brooks Co., model 5280E). In the fore-end of the adsorption column, an in-line static mixer was installed to facilitate mixing. Concentrations of NO and NO<sub>2</sub> that exhausted from

the bypass line and adsorption column were analyzed by using a chemiluminescent  $\text{NO}_x$  analyzer (Thermo Environmental Instruments Inc., model 42C).

DSC, TGA, SEM, EPMA and ToF-SIMS are applied for the identification of species adsorbed and desorbed on the surface. For DSC studies, samples were taken in an aluminium crucible and heated to 600 °C at 10 °C /min. TGA studies were performed at 10 °C/min to 900 °C under a air environment. EPMA was carried out with the accelerating voltage at 20 kV with 1000 times magnification. Time-of-Flight Secondary Ion Mass Spectrometry (ToF-SIMS) analysis was carried out using a system equipped with a two-stage reflectron-type analyzer. A low dose of pulsed  $\text{Cs}^+$  primary ion beam, with an impact energy of 10keV, was employed. The spectrometer was run at an operating pressure of  $10^{-9}$  mbar. The primary ion beam was directed on a square area of  $50 \mu\text{m} \times 50 \mu\text{m}$ . The system was operated in high sensitivity mode with a pulse width of 50 ns and with a beam current of 0.5 nA, resulting in a primary ion dose of approximately  $4 \times 10^{11}$  ions  $\text{cm}^{-2}$  analysis<sup>-1</sup>. SIMS spectra were acquired over a mass range of  $m/z = 1-100$  in negative modes. In this analysis, the background was corrected by measuring and comparing ICP-AES (Labtest Plasmascan, Model 710) and ToF-SIMS. During  $\text{NO}_x$ -adsorbed and desorbed SMAC analyses, tendencies were interpreted by comparison with nonadsorbed SMAC, increasing data credibility.

### **Results and Discussion**

Activated carbon (SMAC) whose surface has been modified with KOH was used in this study. The study examined adsorption and desorption behaviors and the accompanied surface reaction mechanism as well as molecular ions distributed on SMAC. This study found that the presence of a relatively deeper bed depth delays surface oxidation and slows down breakthrough.  $\text{NO}_x$  has become oxidized while inducing three types of physical and chemical bonds during adsorption on SMAC. The product created on the surface after desorption depends on 1) the weak bond between deficient carbon and  $\text{NO}_x$ , 2) decomposition of  $\text{KNO}_2$ , in case of the sample having not been reached the state of complete saturation/surface oxidation, and 3) decomposition of  $\text{KNO}_3$ , which has lost its function as adsorbent. It was confirmed that the adequate temperature suitable for  $\text{NO}_x$  desorption was near 385 °C. It was also observed that potassium remained on the surface even with complete desorption of  $\text{NO}_x$ . SIMS Depth profile of  $\text{OH}^-$  ion was found to decrease sharply after adsorption, and, increased again due to creation of hydrogen bond under desorption. Another finding of the study was that all the new products having been adsorbed on the surface after desorption was  $\text{K}_2\text{O}$ . Figure 1, which is a combination of desorption results, shows a proportion of three types bond in peaks to a total amount of  $\text{NO}_x$  produced.  $\text{NO}_2$  breakthrough occurred with bed depths of 1cm and 2cm. As bed depths of 1cm and 2cm showed a larger number of the adsorbed sites than in the case of bed depth of 9cm, WB(weak bond):SB(strong bond):VSB (very strong bond) was seen to have the ratios of 2.38:3.67:1 and 1.86:2.55:1, respectively. However, with bed depth of 9cm where no  $\text{NO}_2$  breakthrough occurred, WB:SB:VSB indicated the ratio of 0.44:15.1:1. As bed depth, one of the experimental conditions, becomes deeper, VSB and WB created little amount of  $\text{NO}_x$ .

Figure 2 shows SIMS sputter depth profiles of  $\text{NO}_2^-$ ,  $\text{NO}^-$  and  $\text{OH}^-$  ions in non-adsorbed SMAC,  $\text{NO}_x$ -adsorbed SMAC, SMAC after adsorption, which compares the distribution ratios of  $\text{NO}_2^-$ ,  $\text{NO}^-$  and  $\text{OH}^-$  ions. SIMS enables a high sensitive analysis on  $\text{OH}^-$  ions, which serve as selective adsorption sites together with  $\text{NO}$  and  $\text{NO}_2$  (distributed upon adsorption of  $\text{NO}_x$ ). Given this, the analysis may provide us with information on the reactivity between the manufactured SMAC and  $\text{NO}_x$  as well as distribution of adsorbed molecular ion species depending on surface depth. The result of the counts against the depth has been calculated by dividing the count of major ions appearing in detection to the instrument by counts of C, i.e. the basic substance of the sample. Figure 2(a) shows far larger distribution of  $\text{NO}_2^-$  to cover 462 Å on the surface with 68% oxidation of the surface. The overall distribution of  $\text{NO}_2^-$  to reach 1232 Å, i.e. the depth under analysis, was found to be the highest in  $\text{NO}_x$  adsorbed > SMAC > after adsorption in order. It is deemed that the lower distribution of  $\text{NO}_2^-$  after adsorption than SMAC may be attributed to the fact that N functional group, having existed on SMAC, was bonded with surface oxygen and came to be partially desorbed from the surface when temperature increased. In Figure 2(b),  $\text{NO}^-$  is found to be distributed in a larger quantity as the depth reaches 385 Å (under the  $\text{NO}_x$ -adsorbed condition) and is diffused to cover 1232 Å. In contrast to  $\text{NO}_2^-$ ,  $\text{NO}^-$  is generally distributed in a relatively higher proportion to reach as deep as

depth of the surface under the condition of *NO<sub>x</sub>-adsorbed* when compared to other conditions such as *SMAC* or *After adsorption*. This may be interpreted as follows: First, NO was produced upon adsorption; Secondly, such a reaction may occur due to the influence from NO having not reacted or in a form which did not undergo complete oxidation internally due to obstruction by the crystals having been already adsorbed on the outer area of surface or pores. Thirdly, pore blocking may have been resulted as NO<sub>2</sub> contacts with impregnant existed on the external surface at the earliest stage as seen in Figure 2 (a) and (b). Finally, another possibility exists that surface oxygen of the atomic state was bonded with the N functional group-containing SMAC, and, at desorption of the bonded functional group may have produced NO<sup>-</sup> ions. Figure 2(c) shows sputter depth profile of OH<sup>-</sup>. Distribution of OH<sup>-</sup> is found to be the highest in SMAC (*SMAC > After adsorption > NO<sub>x</sub> adsorbed*). On SMAC, OH<sup>-</sup> ions provide selective adsorption sites and react with NO<sub>2</sub>, as seen in Eq. (1), and evaporate into H<sub>2</sub>O. Accordingly, after adsorption of NO<sub>2</sub>, a substantial reduction of OH<sup>-</sup> was observed regardless of surface depths. However, after desorption, OH<sup>-</sup> ions increased on the surface which may be explained by two possibilities: 1) As KOH in SMAC, non-reacted selective adsorption sites, was decomposed, to produce H<sub>2</sub>O upon desorption at a high temperature, and H<sub>2</sub>O evaporated to enable a hydrogen bond between H with O on the surface; and 2) H bond was broken away from some carbon due to a high temperature and H was bonded with O on the surface.

### Referenece

- [1] Lee, Y. W., Choi, D. K., Park, J. W.: *Ind. Eng. Chem. Res.* 40, 3337 (2001).
- [2] Lee, Y. W., Choi, D. K., Park, J. W.: *Sep. Sci. Technol.* 37, 1 (2002).
- [3] Lee, Y. W., Park, J. W., Choi, D. K.: *Carbon* 40, 1409 (2002)
- [4] Lee, Y. W., Choung, J. H., Choi, D. K., Park, J. W.: *Fundamentals of Adsorption*, IK Int. Ltd. 154-161 (2002)
- [5] Lee, Y. W., Park, J. W., Choung, J. H., Choi, D. K.: *Environ. Sci. Technol.* 36, 1086 (2002).
- [6] Lee, Y. W., Park, J. W., Yun, J. H., Lee, J. H., Choi, D. K.: in press, *Environ. Sci. Technol.*
- [7] Lee, Y. W., Park, J. W., Kim, H. J., Park, J. W., Choi, B. W., Choi, D. K.: submitted to *Carbon*.
- [8] Lee, Y. W., Kim, H. J., Choi, D. K., Yie, J. E., Park, J. W.: submitted to *Environ. Sci. Technol.*
- [9] Kim, H. J., Lee, Y. W., Choi, D. K., Na, B. K., Lee, E. I., Park, J. W.: accepted in *J. Korean Society of Environmental Engineers*.
- [10] Thomas, W. J.; Crittenden, B. *Adsorption Technology and Design*, Butterworth Heinmann: Oxford, 1998.
- [11] Ościk, J., Cooper, I. L. *Adsorption*, John Wiley & Sons: New York, 1982.
- [12] Yang, J., Mestl, G., Herein, D., Shlögl, R., Find, J. *Carbon* 38, 729 (2000).
- [13] Illán-Gómez, M. J., Linares-Solano, A., Radovic, L. R., Salinas-Martínez de Lecea, C. *Energy Fuels* 9, 104 (1995).
- [14] Huang, H. Y., Yang, R. T. *J. Catal.* 1999, 185, 286 (1999).
- [15] Mehandjiev, D., Bekyarova, E., Khristova, M. *J. Colloid Interface Sci.* 192, 440 (1997).
- [16] Márquez-Alvarez, C., Rodríguez-Ramos, I., Guerrero-Ruiz, A. *Carbon* 34, 1509 (1996)
- [17] Carabineiro, S.A., Fernandes, F. B., Vital, J. S., Ramos, A. M., Silva, I. F., *Catal. Today.* 54, 559 (1999).
- [18] Bereznitski, Y., Gangoda, M., Jaroniec, M., Gilpin, R. K. *Langmuir* 14, 2485 (1998).
- [19] de la Puente, G., Gil, A., Pis, J. J., Grange, P. *Langmuir* 15, 5800 (1999).
- [20] Dandekar, A., Baker, R. T. K., Vannice, M. A. *J. Catal* 183, 131 (1999).
- [21] Greenwood, N. N., Earnshaw, A. *Chemistry of the Elements* Butterworth Heinmann: Oxford, 1984.
- [22] Chan, L.K, Sarofim, A. F. Beér, J. M. *Combust Flame* 52, 37 (1983).
- [23] Mochida, I., Kuroda, K., Miyamoto, S., Sotowa, C., Korai, Y., Kawano, S., Sakanishi, K., Yasutake, A., Yoshikawa, M. *Energy Fuels* 11, 272 (1997).

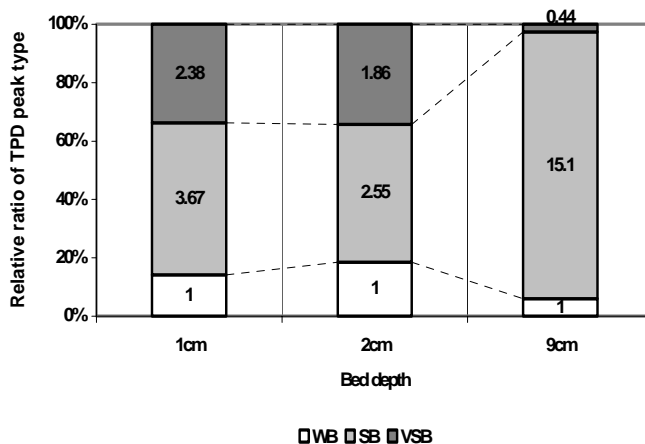


Figure 1. Relative ratio on 3 types bonding strength (WB, SB, VSB) of each peak in NO<sub>x</sub> (NO+NO<sub>2</sub>) concentration profile obtained from Temperature Programmed Desorption when the bed depths of SMAC are (a) 1cm, (b) 2cm, and (c) 9cm.

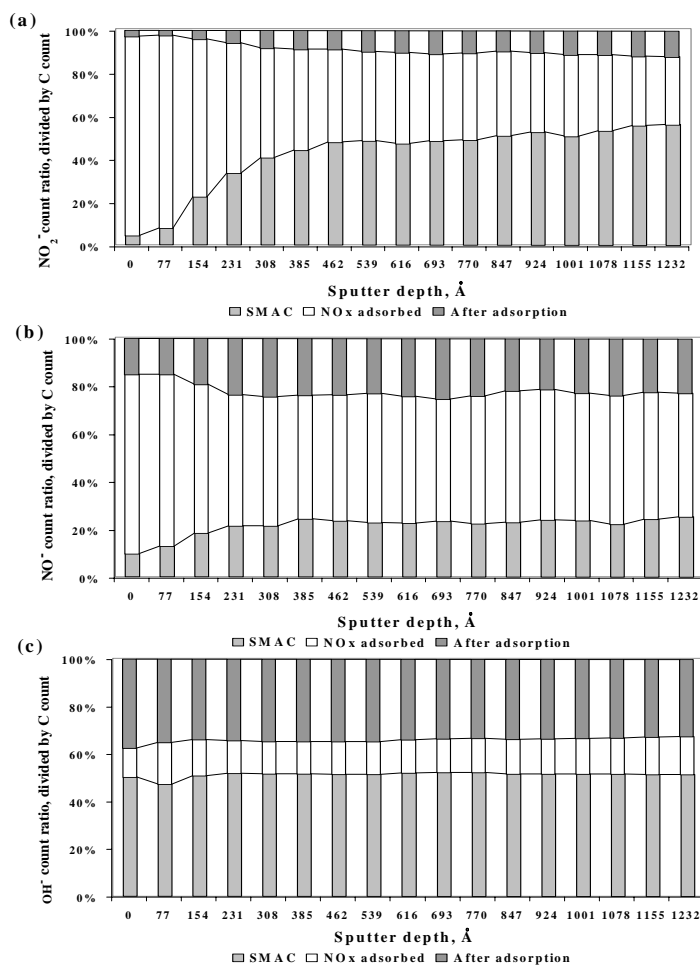


Figure 2. Depth profiles of (a) NO<sub>2</sub><sup>-</sup>, (b) NO<sup>-</sup>, and (c) OH<sup>-</sup> ions in the non adsorbed SMAC and SMAC after NO<sub>x</sub> adsorption and desorption.